

1 A simplified system to quantify storage of carbon dioxide, water vapor and heat within a 2 maize canopy

Taqi Raza^{1*}, Bruce B Hicks^{1,2}, Joel N. Oetting¹ and Neal S Eash¹

5 ¹Department of Biosystems Engineering and Soil Science, The University of Tennessee, Knoxville
6 USA

7 ²MetCorps, Norris, USA

8

⁹ *Corresponding author: Taqi Raza; taqiraza85@gmail.com, traza@vols.utk.edu

10 Department of Biosystems Engineering and Soil Science, The University of Tennessee, Knoxville
11 USA

13 Highlights

14 1. A [unique](#) [new](#) multiport system simplifies measuring CO₂ and water vapor gradients in a
15 plant canopy.

16 2. The system eliminates the effects of sensor calibration differences.

17 3. Field tests illustrate the ruggedness of the design, suitable for remote and demanding
18 circumstances.

19 4. Addition of temperature sensors permits application to surface heat storage and energy
20 [balance](#) [applications](#).

22 Abstract

23 The canopy storage of CO₂, latent heat, and sensible heat within agricultural crops has not yet
24 been fully examined, particularly on small farms situated in complex terrain as commonly found
25 across much of eastern North America and Africa. Reported canopy storage terms are
26 consistently smaller than those found in forest ecosystems, such that they are often
27 neglected. AOur multiport profile system has been developed to examine these storage terms.
28 The system sequentially samples air from four heights to a single non-dispersive Infrared Gas
29 Analyzer (IRGA). Following laboratory testing, the system has been field proven in an east

30 Tennessee [study of a](#) maize crop in 2023. The new system enables quantifications of CO₂[-and](#)
31 latent [and sensible](#) heat atmospheric storage terms and, with supporting temperature
32 measurements, allows improved examination of the surface heat energy budget and the net
33 air-surface exchange of CO₂. [It offers a valuable tool for a better understanding of gas-energy](#)
34 [fluxes on small land-holder farms on topographically varied landscapes.](#)

35

36 **Keywords:** Multi-port system, vertical canopy profile, storage terms (CO₂ and heat), energy
37 balance, maize, carbon sequestration

38

39 **1 Introduction**

40 In the last few decades, significant work has attempted to improve our understanding of
41 gaseous exchanges between soils, plants, and the atmosphere. These improvements have been
42 incorporated in land-surface models and numerically-based weather predictions as well as in
43 assessment of atmospheric fluxes of carbon dioxide (Lamas Galdo et al., 2021), water vapor
44 (Wang et al., 2023), and heat over vegetated landscapes (e.g., Hoeltgebaum and Nelson, 2023).

45 Observations of the surface heat budget over forests have shown that the balance
46 expressed by the familiar relationship:

$$47 R_n - G = H + LE \quad (1)$$

48 Here, R_n is net radiation, G is soil heat flux, H is sensible heat flux and LE is latent heat flux (q.v.
49 Wilson et al., 2002). Measurements of the turbulent fluxes [of](#) H and LE are usually by the eddy
50 covariance (EC) methodology (Nicolini et al., 2018), which is also used to measure the flux of
51 carbon dioxide — F_{CO_2} . In practice, R_n is measured using well-accepted sensors and ground heat
52 flux plates are installed in the soil to determine G . Routine EC measurements are now made at
53 more than 1000 locations globally (c.v. Fluxnet; Pastorello et al., 2020).

54 An important factor emerging from many experimental studies using eddy covariance is
55 that storage terms contribute substantially to energy closure of vegetated areas and to the
56 quantification of evapotranspiration (McCaughy and Saxton, 1988; Hoeltgebaum and Nelson,

57 2023). In concept, errors in the surface heat balance can be attributed to many additional
58 factors, including omission of the heat used in photosynthesis and the storage of heat in plant
59 biomass, in the air below the height of micrometeorological flux measurement and in the soil
60 layer below or above or both the depth of G measurement. If the site in question is not flat,
61 horizontal and homogeneous for a considerable distance upwind, then gravity flows, and
62 advection must be expected to play a role. Investigation of these various contributing factors
63 requires measurement of the relevant variables as they change with space and with time;
64 especially challenging due to temporal (particularly diurnal) changes in air temperature and
65 humidity (Varmaghani et al., 2016) as well as in concentrations of carbon dioxide (herein
66 represented by $[CO_2]$).

67 There are several other possible reasons for energy closure errors in EC
68 experimentation, such as loss of low- or high-frequency flux components, non-optimal
69 coordinate rotation, and the use of inappropriate averaging times (Massman and Lee, 2002;
70 Meyers and Hollinger, 2004; Oetting et al., 2024). Finnigan (2006) reported that the
71 atmospheric heat storage term is underestimated when the average sampling time is large.
72 Neglecting canopy storage terms in studies of Net Ecosystem Exchange (NEE) can also cause
73 substantial errors (Raza et al., 2023). Fewer than 30% of known experimental locations apply a
74 profile measurement system to calculate the temporal variations in storage terms (Papale,
75 2006). Many studies report that energy balance closure is an unsolved problem for a variety of
76 vegetation types: the sum of sensible and latent heat flux is found to be 10-30% lower than the
77 available energy (Wilson et al., 2002; Twine et al., 2000; Leuning et al. 2012; Russell et al. 2015;
78 Raza et al., 2023).

79 In the case of agricultural cropping systems, atmospheric storage terms are usually
80 considered to be small and are often ignored (Nicolini et al., 2018; Raza et al., 2024).
81 Assessments of storage terms within agricultural ecosystems are few and differ from those well
82 documented by researchers in the case of forest ecosystems studies (Mayocchi and Bristow,
83 1995; Wilson et al., 2002; Hicks et al., 2020). Most results of heat storage in forest
84 environments focus on the atmospheric component of the total heat storage.

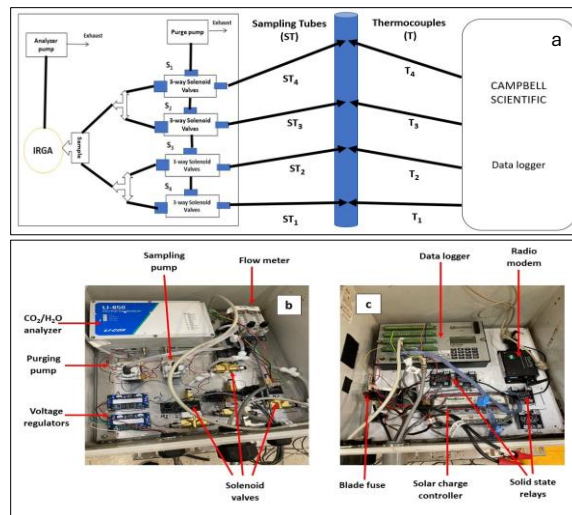
85 These present paper focusses on the a resolution to needs for detailed measurements of
86 profiles of water vapor and carbon dioxide profiles and concentrations in the atmospheric
87 surface roughness layer, as arose in the decade-long sequence of field studies conducted by the
88 University of Tennessee in Lesotho, Zimbabwe, Ohio and Tennessee (see Eash et al., 2013;
89 O'Dell et al., 2014, 2015; Hicks et al., 2021, 2022 Eash et al., O'Dell et al; Hicks et al.). The surface
90 roughness layer is that layer of air in contact with the surface below the height at which familiar
91 micrometeorological flux/gradient relationships apply. These studies have concentrated on
92 aspects of the surface energy balance and crop carbon dioxide exchange in areas different from
93 conventional agricultural-meteorology experiments, namely in areas of complex terrain and
94 small plots as confront common in farming communities in Africa and much of eastern North
95 America. These experiments have increasingly indicated the importance of detailed
96 temperature and concentration measurements in the surface roughness layer.

97 A central requirement has been the need to describe water vapor and CO₂
98 concentrations in more detail than conventional micrometeorology normally provides. To this
99 end, the present paper describes an experimental procedure that builds upon air-sampling
100 systems of the past but is streamlined to provide the requisite measurements with the desired
101 time and space detail, in areas often distant from immediate technical support. Some
102 illustrations of its field utility are provided, using observations from a study of a maize canopy in
103 eastern Tennessee in 2023.

104 **2. Apparatus design and operation**

105 The measurement system development described here is an outgrowth of experience with eight
106 preceding field studies, conducted at locations in Lesotho, Zimbabwe, Tennessee, and Ohio
107 (Eash et al., 2013; O'Dell et al., 2014, 2015; Hicks et al., 2021, 2022). These demonstrated the
108 need for a reliable yet technically simple system to measure gas concentrations within and
109 above a growing crop. To satisfy the basic requirements for time continuity and reliability of the
110 data record, a new multi-port sampling system was developed.

111 To avoid consequences of individual sensor offsets when gradients are computed, the
 112 new system is designed to use a single detection system, in this case an infrared $\text{CO}_2/\text{H}_2\text{O}$ gas
 113 analyzer (IRGA; LI-COR-850, Lincoln, NE). Figure 1 presents a schematic description of the
 114 apparatus. The system is designed to maintain continuous airflow through all intake tubes, to
 115 cycle through all heights of measurement in one minute (7.5 seconds for each height) and to
 116 minimize the switching time between samplings. ~~The system uses two small pumps [Model TD-31SA, Brailford & CO, Inc. Antrium, NH, USA], one pump (the purge pump) draws in air at a~~
 117 ~~constant rate through all intake tubes to minimize hygroscopic interactions along the tube~~
 118 ~~walls. Another pump (the sampling pump) pushes the drawn air to the IRGA. The sampling~~
 119 ~~pump is mounted close to the IRGA so that air smoothly enters the IRGA at ambient pressure.~~
 120 ~~When sampling the airflow through a specific tube the flow rate is maintained at 1000 ml min^{-1} .~~
 121 ~~The flow rates through the other three tubes are then maintained at 700 ml min^{-1} by flow~~
 122 ~~meters [LZQ-7 flowmeter, 101.3 KPa, Hilitand, China]. The switching between sampling tubes is~~
 123 ~~controlled by four three way brass and stainless steel solenoid valves [231Y-6, Ronkonkoma,~~
 124 ~~NY, USA].~~
 125



126

127 Fig. 1. Details of the multi-port sampling system: (a) schematic diagram of the manifold for
128 profile sampling of CO₂ and H₂O, (b) a photograph of the analyzer, pump, and manifold
129 system, (c) the data logger for data collection.

130 The system uses two small pumps [Model TD-3LSA, Brailsford & CO., Inc. Antrium, NH,
131 USA], one pump (the purge pump) draws in air at a constant rate through all intake tubes to
132 minimize hygroscopic interactions along the tube walls. Another pump (the sampling pump)
133 pushes the drawn air to the IRGA. The sampling pump is mounted close to the IRGA so that air
134 smoothly enters the IRGA at ambient pressure. When sampling the airflow through a specific
135 tube the flow rate is maintained at 1000 ml min⁻¹. The flow rates through the other three tubes
136 are then maintained at 700 ml min⁻¹ by flow meters [LZQ-7 flowmeter, 101.3 KPa, Hilitland,
137 China]. The switching between sampling tubes is controlled by four three-way brass and
138 stainless-steel solenoid valves [231Y-6, Ronkonkoma, NY, USA].

139 Each sampling tube ~~is~~is same length (10.5 m) long, to ensure samples from each
140 sampling height have the same transit time. The purge pump manifold and all sampling tubes
141 are constructed of the same kind of urethane [BEV-A-LINE, Polyethylene material, Cole-Parmer,
142 City, State]. Before entering the analyzer, the air is passed through a 1-μm pore filter [LI-6262,
143 LI-COR, Lincoln NE, USA] to avoid the accumulation of debris, dirt, particles, etc., that can cause
144 contamination in the analyzer optical cells. The air outlet of the purge pump and IRGA are open
145 directly to the atmosphere. Digitizing is at 5 Hz frequency. The data system is arranged to
146 record averages and standard deviations at a pre-arranged periodicity, depending on the
147 research goal but typically 5, 10 or 15 minutes.

148 The performance of the system for measurement of CO₂ and H₂O profiles was examined
149 extensively before its field deployment. The apparatus was first flushed with nitrogen (N₂) gas
150 to create a zero-carbon dioxide environment. Subsequently, a known concentration of CO₂ (430
151 ppm) at ambient pressure was fed through the intake tubes sequentially and system outputs
152 were measured. This process allowed determination of the time neededtaken to reach stable
153 measurement readings.

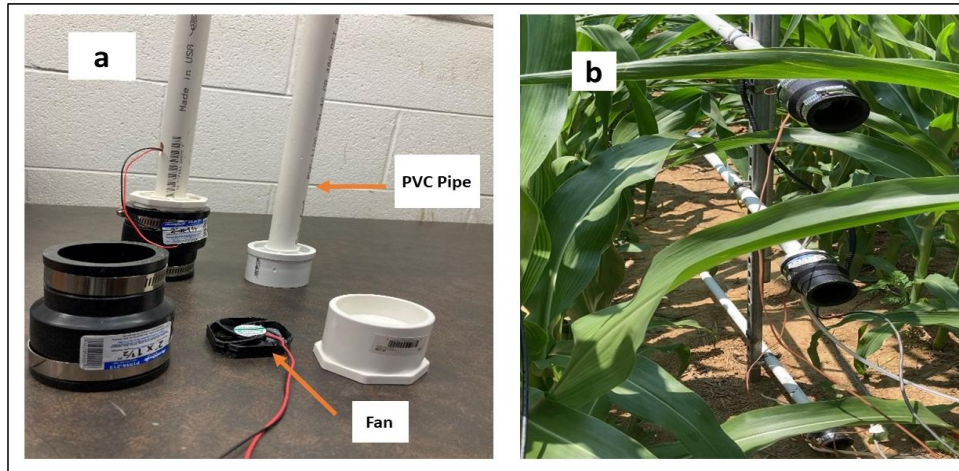
154 To derive a continuous record of concentrations at each height of interest (in the
155 preliminary configuration, four of them), switching between heights was set at every 7.5
156 seconds allowing each of the heights to be sampled twice in every minute. The laboratory tests
157 showed that after the IRGA received a step change in CO₂ concentration, it took approximately
158 1.8 seconds to achieve a steady output. During the laboratory evaluation period, the recorded
159 error was less than 0.5% in [CO₂] between sampling heights. An accuracy error of less than 1%
160 is well within the acceptable range for the IRGA now used according to the specifications
161 provided by the manufacturer and much less than higher errors common in measurements of
162 this kind (Montagnani et al. 2018)

163 **3. Field evaluation**

164 An ongoing field study of a maize crop in East Tennessee provided an opportunity to test the
165 new sampling system in experimentally demanding circumstances. The experiment was
166 conducted at a 23 ha plot of agricultural farmland, near Philadelphia, in Loudon County
167 Tennessee (35.673° N, 84.465° W). The site is typical ~~of~~ agricultural land used for mainly maize
168 and soybean production, in slightly rolling terrain that presents a challenge to EC
169 measurements, with local slope varying from 1% to 5% depending on location. For the present
170 purpose, it is not necessary to provide details of the experiment or of the analysis resulting
171 from it. Such detailed examination of the observations will be presented elsewhere. However,
172 the maize variety was "Dekalb 66-06". The mean annual temperature and precipitation of the
173 site are 13.5 °C and 140 cm respectively. The soil was classified as an Alcoa Loam (fine, thermic
174 Rhodic Paleudult) according to the USDA-NRCS (2018). The experiment extended through the
175 entire growth cycle, from which data for six weeks during the months of May and June 2023
176 have been extracted for the present illustrative purpose. Maize planting was on 25 April with
177 Dekalb hybrid hybrid 66-06 at a density of approximately 81,000 plants per ha, the, so that the
178 illustrations to follow relate to a period of rapid growth of the canopy, from soon after
179 emergence (in early May) to tasseling (in June).

180 In the field test considered here, the system was used to measure at heights of 0.11 m,
181 0.5h, 1+h, 2+h, where h is maize canopy height (in meters) above the soil surface. Note that one

182 intake was permanently set at 0.11 m, and the three other heights were adjusted as the maize
183 grew. Sampling intakes were positioned on a 3.5 m steel mast. Thermocouples at the same
184 height as gas sample intakes were used to measure temperature gradients; these were
185 aspirated within a white PVC pipe shield of 1.9 cm diameter (Figure 2a) that also served as a
186 radiation shield.

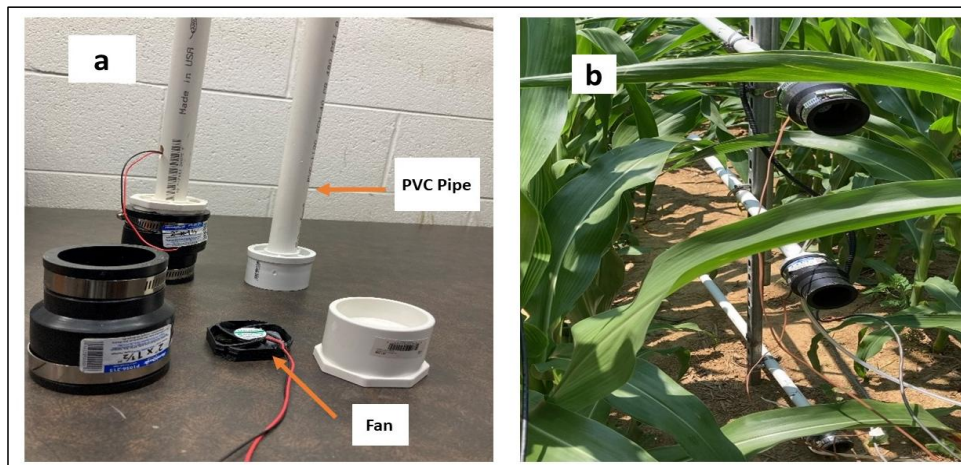


187
188 Fig. 2. (a) Installation components at each height of the new profile system, showing the
189 aspirated CO₂ intake tubes and thermocouples. (b) Deployment in a maize canopy; the two
190 lowest heights are shown.

191
192 The experimental program hosting this field test utilized Two tripods and a horizontal
193 bar supported a tripod tower to support an eddy covariance system (adjusted as the crop grew
194 to maintain a height about 2 m above the crown) and supporting micrometeorological
195 measurements — an IRGASON [CO₂/H₂O] open path gas analyzer system, [Campbell Scientific,
196 Logan, Utah], a net radiometer [Kipp & Zonen, OTT HydroMet B.V. Delft, Netherlands], infrared
197 radiometers [IRs-S1-111-SS, Apogee Instruments Inc, City, State, USA], and type T
198 thermocouples [Omega, City, State, USA]. The entire observational system was visually
199 inspected every week for signs of leakage, condensation, and contamination. The IRGASON gas

200 analyzer used for eddy covariance was independent of the IRGA used for concentration
201 gradient measurements. The availability of the EC system and its supporting measurements
202 enabled the tests of the new sampling system to extend to investigation of such matters as the
203 height of origin of thermal eddies, as will be reported later.

204



205
206 ~~Fig. 2. (a) Installation components at each height of the new profile system, showing the~~
207 ~~aspirated CO₂ intake tubes and thermocouples. (b) Deployment in a maize canopy; the two~~
208 ~~lowest heights are shown.~~

209 **3.1. Results — CO₂**

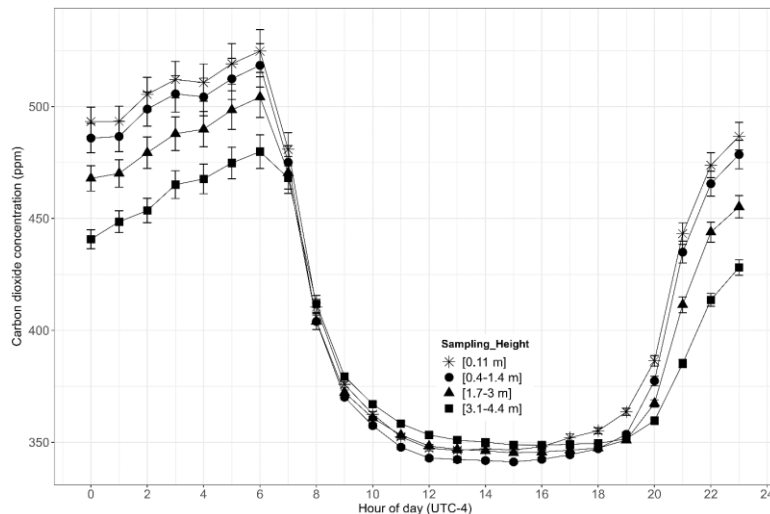
210 Within a nocturnal strongly stratified surface roughness layer, previous experiments have
211 revealed the ubiquity of pooling of CO₂ emitted by soil biota and root respiration. Fig. 3
212 presents average diurnal cycles of CO₂ concentrations measured over the six weeks from 18
213 May to 29 June at four heights, two within the canopy and two above. Error bounds correspond
214 to +/- one standard error of the mean.

215

216 The variability of CO_2 was found to be higher at nighttime than in daytime. The greatest
217 variability was recorded within the canopy, at height 1 (0.11 m) and height 2 (0.4–1.4 m).

218 The observations confirm the generally accepted features of nocturnal accumulation of
219 CO_2 effluxes from the soil but with detail sufficient to warrant detailed examination. The close
220 tracking of the records for the different measurement heights provides confidence in the
221 performance of the sampling system and indicates that the same causative mechanisms affect
222 all of the heights similarly. The nighttime results that are plotted support the assumptions
223 made elsewhere that changes in the surface impacts the stratified atmosphere above, are
224 mostly in accord with expectations of CO_2 profile linearity (Galmiche and Hunt, 2002; Verma
225 and Rosenberg, 1976), a result that is supported by close examination of CO_2 averages over
226 shorter nighttime periods.

227



228

229 Fig. 3. Average diurnal cycle of CO_2 obtained using the new system described here, for
230 the six weeks. Symbols correspond to different heights of measurements with error bars
231 corresponding to +/- one standard error.

232 The variability of CO₂ was found to be higher at nighttime than in daytime. The greatest
233 variability was recorded within the canopy, at height 1 (0.11 m) and height 2 (0.4 – 1.4 m).

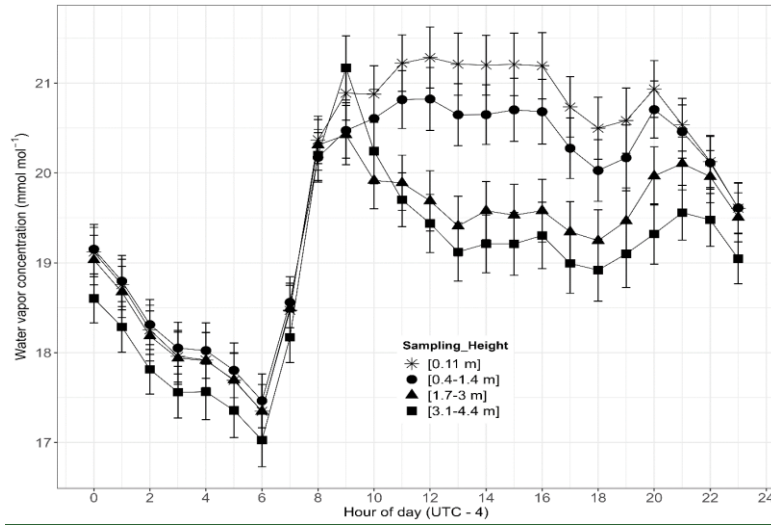
234 The observations confirm the generally accepted features of nocturnal accumulation of
235 CO₂ effluxes from the soil but with detail sufficient to warrant detailed examination. The close
236 tracking of the records for the different measurement heights provides confidence in the
237 performance of the sampling system and indicates that the same causative mechanisms affect
238 all of the heights similarly. The nighttime results that are plotted support the assumptions
239 made elsewhere that changes in the surface impacts the stratified atmosphere above, are
240 mostly in accord with expectations of CO₂ profile linearity (Galmiche and Hunt, 2002; Verma
241 and Rosenberg, 1976), a result that is supported by close examination of CO₂ averages over
242 shorter nighttime periods.

243 Following 0600 local time (LT), about the average time of sunrise, the average
244 concentrations of CO₂ dropped rapidly as photosynthesis commenced and as convection
245 started to mix surface air with the overlying atmosphere. At all heights this initial decrease was
246 followed by a more rapid loss rate until concentrations dropped to about 350 ppm in the
247 afternoon (1200 to 1800 LT), much lower than ambient concentrations thereby reflecting the
248 efficiency with which the maize crop extracted CO₂ from the air. Near sunset, [CO₂] started to
249 increase and continued to build until reaching maximum values immediately before dawn.
250 Concentrations within the canopy do not differ significantly, although the 0.11 m height values
251 always exceed those further above the soil surface. In general, [CO₂] decreased with increasing
252 height. All of these observations align well with contemporary views of the post-sunrise
253 initiation of photosynthesis and its continuation through the following daylight hours.

254 The nocturnal accumulation of CO₂ observed here is not unusual. In many climatic
255 regions, nighttime soil temperatures remain high enough to sustain microbial and soil
256 respiration activities, resulting in CO₂ accumulation in the stratified air above the ground. After
257 the sun rises, increased light availability increases stomatal activity and photosynthesis rates.

258 **3.2. Results — H₂O**

259 As in Fig. 3, Fig. 4 shows the average diurnal cycle constructed from 15-minute H_2O
260 concentration observations. At all heights a sharp increase in $[\text{H}_2\text{O}]$ was recorded in the
261 morning at the same time as the sudden decrease for $[\text{CO}_2]$ seen in Fig. 3.

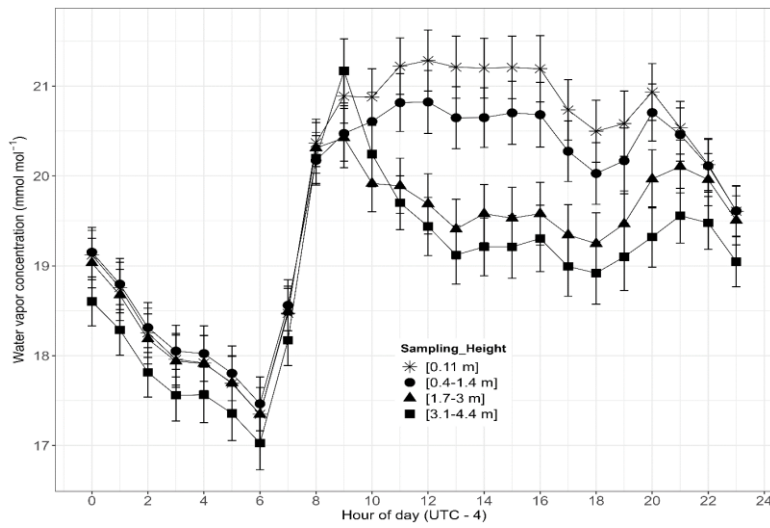


263

264 Fig. 4. Average diurnal cycle of the vertical profile of water vapor concentration
265 averaged over six weeks as in Figs. 3. Symbols correspond to different heights of
266 measurements with error bars corresponding to +/- one standard error.

267 Subsequently, $[\text{H}_2\text{O}]$ peaked at about 0900 LT and, within the canopy, maintained this
268 concentration throughout the daylight hours. Above the canopy, average concentrations
269 decreased and a different concentration constancy was attained. After the period around
270 sunset had passed, at about 2000 LT, $[\text{H}_2\text{O}]$ started decreasing approximately linearly with time
271 until sunrise approached. The H_2O concentration generally decreased as the measurement
272 height increased for both day and night because a constant source of water vapor was the soil
273 surface, with crop evapotranspiration adding H_2O in the daytime. Dewfall is expected to be
274 important, a contribution that can be uniquely addressed using the new sampling system.

275 Figures 34 and 45 reveal considerably different cycles of CO₂ and H₂O. At night, Fig. 3
276 shows a more striking [CO₂] gradient than does Fig. 4 for [H₂O]. The reason is presumed to be
277 that CO₂ continues to be emitted from the soil at night and accumulates within the stratified
278 layer of air, whereas there is no parallel process influencing H₂O concentrations. In daytime,
279 there is little consistent [CO₂] gradient information derivable from Fig. 3, but for [H₂O] in Fig. 4
280 there is a clearly visible [H₂O] gradient structure. This suggests a slow-down of CO₂ exchange in
281 the afternoons while evaporation continued.



283

284 **Fig. 4. Average diurnal cycle of the vertical profile of water vapor concentration**
285 **averaged over six weeks as in Figs. 3. Symbols correspond to different heights of**
286 **measurements with error bars corresponding to +/- one standard error.**

287 The processes of evaporation from the soil surface and evapotranspiration from leaves are
288 linked with solar radiation. Overall, the present results highlight changes in the vertical
289 distribution of water vapor and its temporal variability, indicating near simultaneity of changes
290 on CO₂ and H₂O concentrations following dawn (compare Figs. 3 and 4).

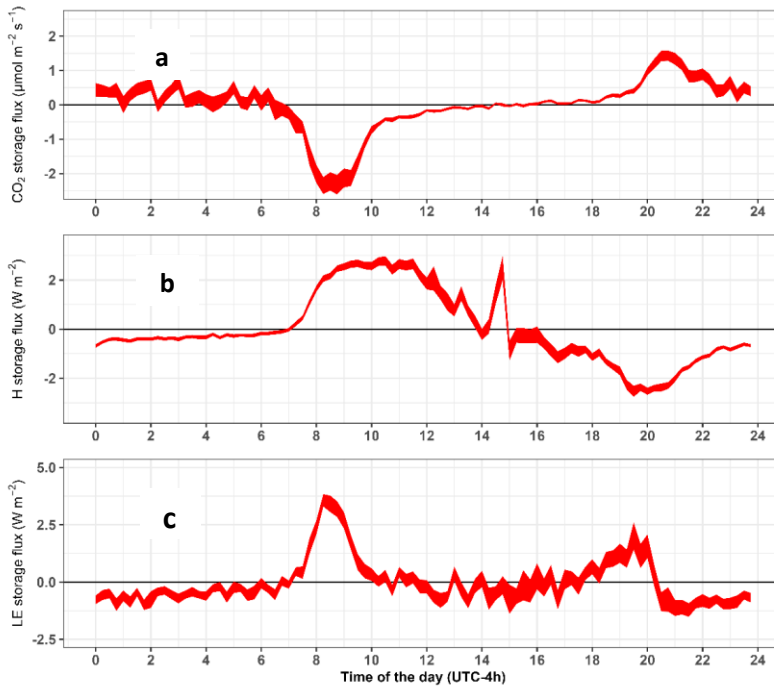
291 **Results — atmospheric storage**

292 The vertical profile data can also be used to explore how various atmospheric storage fluxes
293 influence the CO₂ status and energy budget of the maize crop. In accordance with many
294 studies of the surface energy budget using EC systems, atmospheric storage terms refer to
295 depletion or accumulation of scalar quantities (CO₂, H₂O, etc.) in a hypothetical control volume
296 beneath the height of turbulent flux measurement by EC. A storage flux is defined as the rate
297 of change of dry molar concentrations of the same variables within the same control volume.
298 Both concepts relate most directly to the conditions of “perfect” micrometeorology. In
299 practice, natural complexities of surroundings and exposures interfere to the extent that
300 measurements will be site-specific. Moreover, the covariances are statistical quantities, with
301 well-recognized error margins associated with every quantification of them. During this study,
302 the storage fluxes of scalar quantities (CO₂, water vapor, etc.) were calculated using the ICOS
303 ([Integrated Carbon Observation System](#)) methodology (Montagnani et al., 2018). For the case
304 of CO₂,

$$305 \quad J_c = \overline{\rho_d} \sum_{i=1}^N \left(\frac{\Delta c}{\Delta t} \right)_i \Delta z_i \quad (2)$$

307

308 Here, J_c is the storage term of CO₂ (for example) within the i^{th} layer over which Δc is measured,
309 Δz_i is the thickness of this layer and Δt is the measurement time step; ρ_d is dry air density, and
310 N is the number of layers (number of measurements points). To calculate the storage terms as
311 described by Eq. 2, raw data were averaged into 15-minute periods, yielding the results plotted
312 in Fig. 5.



313

314

315

316 Fig. 5. Diurnal patterns of CO₂ atmospheric storage (a), sensible heat storage (b) and

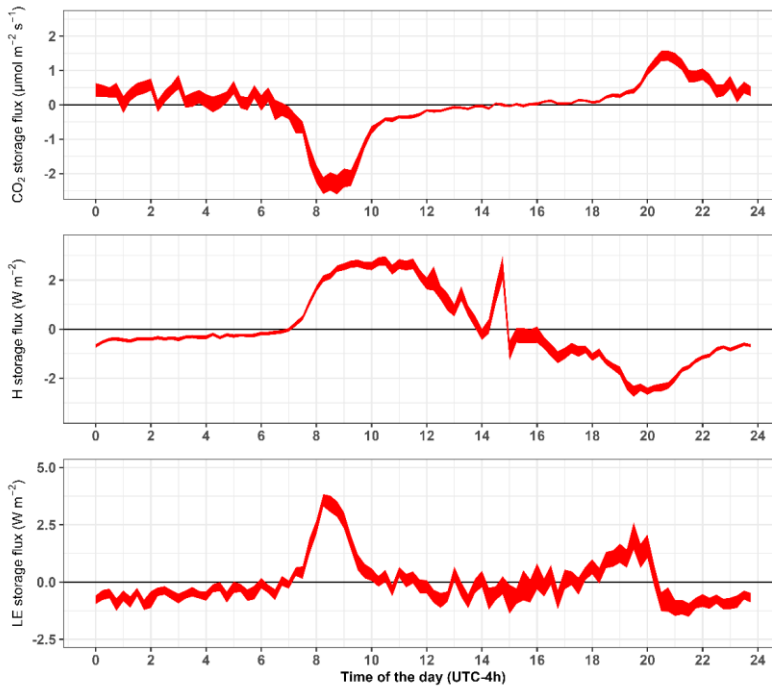
latent heat storage (c) of the maize crop in early stages of growth (see Table 1 a-b). The
widths of the traces correspond to +/- one standard error on the means.

317

318 CO₂ storage (Fig. 5a) exhibited a larger magnitude and more variation at nighttime compared to
 319 daytime, due to the CO₂ pooling and the intermittency of incursions from air aloft. During the
 320 night, photosynthesis did not occur, and CO₂ emitted from the soil accumulated in the overlying
 321 stratified atmosphere (Ryan and Law, 2005; Davidson and Janssens, 2006). Soon after sunrise,
 322 the nighttime stratification began to weaken, and photosynthesis commenced. The trapped CO₂
 323 was consumed by photosynthesis and mixed with air above the canopy as unstable
 324 stratification evolved. Minimal CO₂ storage during the daytime can be due to the instability and
 325 which the vegetation was exposed. More efficient exchange between plant and atmosphere

326 then results in low storage of CO₂ in the air space below the uppermost height of [CO₂]
327 measurement. At night, subcanopy ventilation by intermittent gusting results in a large
328 variation between negative and positive CO₂ storage.

329 Observations such as these are facilitated by the profile sampling system now
330 advocated. In the future, it is planned to use the new capability to revisit the quality assurance
331 methodology of EC determinations by comparing atmospheric storage to the statistical
332 uncertainty of the covariances. In this context, note that Fig. 5b indicates sensible heat
333 atmospheric storage terms equivalent, on average, to about 2 W m⁻² in the late morning,
334 followed by a downward trend through the afternoon until reaching a minimum a few hours
335 after sunset. The irregularity seen soon after noon is presently unexplained. Clearly, individual
336 shorter-term averages could display greater averages and increased scatter, but this remains to
337 be explored. In comparison, Finkelstein and Sims (2001) derive uncertainties associated with
338 30-min EC evaluations of the sensible heat covariance in the range 5% to 10% in daytime.



339

340 Fig. 5. Diurnal patterns of CO_2 atmospheric storage (a), sensible heat storage (b) and latent heat
 341 storage (c) of the maize crop in early stages of growth (see Table 1 a-b). The widths of the traces
 342 correspond to ± 1 standard error on the means.

Formatted: Normal, Centered, Indent: Left: 0", Space Before: 12 pt

343 The nocturnal sensible (Fig. 5b) and latent (Fig. 5c) heat energy storages remained low
 344 and slightly negative until sunrise, about 0600 LT. As the air cooled during the night, sensible
 345 heat storage in the air mass remained slightly negative as its temperature decreased. After
 346 sunrise, the air mass warmed and the sensible heat storage rose to a maximum value of about 2
 347 W m^{-2} between 1200 LT and 1230 LT. Afterwards, the sensible heat storage rate declined,
 348 reaching negative values a few hours before sunset and attaining a minimum value (about -1.5
 349 W m^{-2}) a few hours before midnight. The sensible heat storage subsequently trended to near-
 350 zero constancy until being disrupted by sunrise at about 0700 LT.

351 Latent heat storage (Fig. 5c) fluctuated near zero for most of the daylight hours, after
352 exhibiting a major positive excursion ($> 4 \text{ W m}^{-2}$) during the few hours after sunrise. After about
353 2100 LT, latent heat storage fluctuations like the variations seen in Fig. 5a occurred until
354 sunrise, with an average of about -0.5 W m^{-2} . Comparison with Fig. 5a indicates that the post-
355 sunrise increases in latent heat storage coincided with the decrease in CO_2 storage. The
356 sensible heat storage appears to have been delayed by a fraction of an hour. Interpretation of
357 these observations requires consideration of dewfall and its evaporation.

358 Table 1-~~a-b~~ lists some of the plant growth characteristics during the six-weeks
359 considered here. Also listed are the magnitudes of maximum and minimum storage terms
360 during each of the sampling periods, shown here to exemplify the ability of the new sampling
361 system to reveal such extremes. Detailed examination of the plant-atmosphere interaction for
362 the entire growing season will be presented elsewhere. During the six-week evaluation period,
363 CO_2 atmospheric storage increased as the plant grew and as the soil warmed (increasing
364 subsurface heterotrophic CO_2 generationsubsurface) but not substantially; the highest storage
365 rate was found at the VT (tasseling) stage and the minimum at the V2 growth stage, five weeks
366 earlier. Similarly, latent heat storage increased significantly, presumably due to increasing leaf
367 area and transpiration. Latent and sensible heat storage was found higher in the VT growth
368 stage than in other growth stages. As the crop grew, different processes became prominent
369 causes of the storage of energy and CO_2 . When the maize was in its early growth stage, the
370 canopy was not fully developed, the soil was cooler, and CO_2 storage did not show much
371 change. However, there were substantial variations in the sensible and latent energy storage
372 terms as the crop grew (see Table 1-~~a-b~~).

373 **Table 1-~~a-b~~**. Height adjustment during the crop growth stage and maximum and minimum
374 storage terms. V1 is the first leaf emergence, Vn is when the n^{th} leaf fully emerged, and VT is the
375 tasseling stage. Height 1 (H_1) was kept constant throughout the experiment while the other three
376 heights (H_2 , H_3 , and H_4) changed as the plants grew. Negative and positive signs represent the
377 2.5th percentile (minimum) and 97.5th percentile (maximum) quartile values observed during the
378 different periods.

Table	Measurement height (m)	Growth stage	Latent heat storage	Sensible heat storage	CO ₂ Storage	Average precipitation	Average Temperature	
Date	H ₁	H ₂	H ₃	H ₄	W m ⁻²	W m ⁻²	mm	°C
May 15-May 21	0.11	0.43	0.60	2.00	V2-V3	-15.19 to 6.13	-5.67 to +2.59	
May 22-May 28	0.11	0.43	0.60	2.00	V3-V4	-19.45 to +8.16	-5.67 to +3.21	
May 29-June 4	0.11	0.43	1.72	3.07	V5-V6	-19.72 to +8.95	-11.65 to +3.74	
June 5-June 11	0.11	0.75	2.10	3.12	V6-V7	-19.72 to +9.01	-45.65 to +4.07	
June 12-June 18	0.11	0.95	2.50	3.36	V7-V8	-22.72 to +9.36	-45.65 to +3.68	
June 19-June 25	0.11	1.27	3.00	4.36	V7	-22.73 to +9.38	-15.33 to +4.84	
							0.00	19.22-26.46

Table 1-a	Measurement height (m)	Growth stage	Latent heat storage	Sensible heat storage			
Date	H ₁	H ₂	H ₃	H ₄		W m ⁻²	W m ⁻²
May 15-May 21	0.11	0.43	0.60	2.00	V2-V3	-15.19 to 6.13	-5.67 to +2.59
May 22-May 28	0.11	0.43	0.60	2.00	V3-V4	-19.45 to +8.16	-5.67 to +3.21
May 29-June 4	0.11	0.43	1.72	3.07	V5-V6	-19.72 to +8.95	-11.65 to +3.74
June 5-June 11	0.11	0.95	2.50	3.36	V6-V7	-19.72 to +9.01	-45.65 to +4.07
June 12-June 18	0.11	0.95	2.50	3.36	V7-V8	-22.72 to +9.36	-45.65 to +3.68
June 19-June 25	0.11	1.27	3.00	4.36	V7	-22.73 to +9.38	-15.33 to +4.84

380

Table 1-b	Measurement height (m)				Growth stage	CO ₂ -Storage	Average precipitation	Temperature
Date	H ₁	H ₂	H ₃	H ₄		μmol m ⁻² s ⁻¹	mm	°C
May 15-May 21	0.11	0.43	0.60	2.00	V2-V3	-7.12 to +2.78	0.00	14.90-25.74
May 22-May 28	0.11	0.43	0.60	2.00	V3-V4	-7.12 to +2.87	0.031	14.59-26.63
May 29-June 4	0.11	0.43	1.72	3.07	V5-V6	-9.51 to +2.59	0.007	14.17-28.12
June 5-June 11	0.11	0.75	2.10	3.12	V6-V7	-9.67 to +2.33	0.165	12.87-29.70
June 12-June 18	0.11	0.95	2.50	3.36	V7-V8	-9.68 to +2.36	0.081	13.41-29.12
June 19-June 25	0.11	1.27	3.00	4.36	V8	-6.23 to +2.57	0.00	19.22-26.46

381

382

383

384 **4. Conclusions**

385 The field evaluation of the multi-port profile system demonstrated its effectiveness in
 386 measurement of CO₂ and H₂O concentrations at different heights within the surface roughness
 387 layer. The multiple-height profile system aided substantially to understanding CO₂ and H₂O
 388 concentration variations and their vertical profiles, thereby facilitating precise assessments of
 389 their exchanges, storage, and overall balance within the growing maize ecosystem. The
 390 observations reveal that different processes became prominent at different growth stages,
 391 which influenced the atmospheric storage of heat energy and gas and the associated fluxes as
 392 the canopy developed. An issue remaining to be addressed is that condensation of water in the
 393 sampling tubes was sometimes observed; this will affect measurement accuracy and steps to
 394 eliminate the problem are presently being reviewed.

395 The 2023 field experience with the new system indicates that canopy data obtained
 396 from the vertical profile observations offer potential for many applications in future studies
 397 such as evaluation of soil-plant-atmospheric models that rely on the precise estimation of CO₂,
 398 heat and water vapor fluxes. Note that the definition of the heat storage used here (as in Eq.

399 (2)) omits warming of the biomass. This omission accounts for the differences between the
400 storage terms now computed and those published previously (e.g., Hicks et al., 2022).

401 The simplicity of the sampling system device contributes to its success — it suffered a
402 few disruptions during the testing period. This new measurement system will be employed in
403 future studies of air-surface exchange when moderated by the presence of a crop and
404 especially when operation in remote locations is required. It requires less power, a single IRGA
405 and has a low maintenance cost as compared to traditional systems (e.g. EC). These features
406 reduce operation complexity and maintenance requirement, making it more suited for resource
407 limited or remote locations, particularly small farms holder. Measurements made will permit
408 improved quantification of storage terms — atmospheric, biological, in the soil, and all
409 contributing to a better understanding of the surface heat energy balance. Sub-canopy
410 measurements, in particular, will will help track how respiration, evaporation, photosynthesis,
411 etc. vary through the depth of the canopy. Such studies will also help to evaluate
412 micrometeorological models, such as those describing the variation of gases, temperature, and
413 water vapor within a canopy. This new device is now being used for the assessment of canopy
414 gas emissions, starting with carbon dioxide but in the future studies will intended to include
415 nitrous oxide. In summary, this new device has the potential to improve our understanding of
416 soil-plant-atmosphere interactions, particularly within the plant canopies.

417 **Author contribution statement**

418 **TR:** Data curation, Formal analysis, Methodology, Visualization, Writing – original draft. **BBH:** Supervision,
419 Methodology, Visualization, Writing – revision and editing. **NSE:** Supervising, Funding acquisition, Project
420 administration, Writing – review & editing. **JNO:** Formal analysis, writing and reviewing.

Formatted: Font: 12 pt

Formatted: Font: 12 pt

421 **Funding**

422 This work was supported by DuPont Tate & Lyle Bio Products Company.

Formatted: Font: 12 pt

423 **Declaration of competing interest**

424 Authors declare no competing interest associated with this submission.

Formatted: Font: 12 pt

425 **Acknowledgment**

426 This work was supported by the University of Tennessee, Knoxville. The authors thank David R.
427 Smith (Senior Technical Specialist, BESS, UTK), Wesley C. Wright (Senior Research Associate,
428 BESS, UTK), Scott Karas Trucker (Senior Technical Specialist, BESS, UTK) and Josh Watson
429 (Farmer) for their support.

430 **References**

431 Davidson, E., and Janssens, I.: Temperature sensitivity of soil carbon decomposition and
432 feedbacks to climate change. *Nature*, 440, 165–173,
433 <https://doi.org/10.1038/nature04514>, 2006.

Formatted: Font: (Default) +Headings (Calibri), 12 pt

434 Eash, N.S., O'Dell, D., Sauer, T.J., Hicks, B.B., Lambert, D.L. and Thierfelder, C.: Real-time carbon
435 sequestration rates on smallholder fields in Southern Africa. Institute of Agriculture,
436 University of Tennessee, Knoxville, TN., 2013.

Formatted: Font: (Default) +Headings (Calibri), 12 pt

Formatted: Font: (Default) +Headings (Calibri), 12 pt

437 Finkelstein, P.L. and Sims, P.F.: Sampling error in eddy correlation flux measurements. *J.*
438 *Geophys. Res.: Atmospheres*, 106(D4), 3503–3509,
439 <https://doi.org/10.1029/2000JD900731>, 2001.

Formatted: Font: (Default) +Headings (Calibri), 12 pt

440 Finnigan, J.: The storage flux in eddy flux calculations, *Agric. For. Meteorol.*, 136(3–4), 108–113,
441 <https://doi.org/10.1016/j.agrformet.2004.12.010>, 2006.

Formatted: Font: (Default) +Headings (Calibri), 12 pt

Formatted: Font: (Default) +Headings (Calibri), 12 pt

442 Galmiche, M. and J. C. R. Hunt.: The formation of shear and density layers in stably stratified
443 turbulent flows: linear processes. *J. Fluid Mech.*, 455, 243–262,
444 <https://doi.org/10.1017/S002211200100739X>, 2002.

Formatted: Font: (Default) +Headings (Calibri), 12 pt

445 Hicks, B.B., Eash, N.S., O'Dell, D.L. and Oetting, J.N.: Augmented Bowen ratio analysis I: site
446 adequacy, fetch and heat storage (ABRA), *Agric. For. Meteorol.*, 290, 108035,
447 <https://doi.org/10.1016/j.agrformet.2020.108035>, 2020.

Formatted: Font: (Default) +Headings (Calibri), 12 pt

Formatted: Font: (Default) +Headings (Calibri), 12 pt

448 Hicks, B.B., Lichiheb, N., O'Dell, D.L., Oetting, J.N., Eash, N.S., Heuer, M. and Myles, L.: A
449 statistical approach to surface renewal: The virtual chamber concept. *Agrosys. Geosci.*
450 *Environ.*, 4(1), p.ee20141, <https://doi.org/10.1002/agg2.20141>, 2021.

Formatted: Font: (Default) +Headings (Calibri), 12 pt

451 Hicks, B.B., Oetting, J.N., Eash, N.S. and O'Dell, D.L.: Augmented Bowen ratio analysis, II: Ohio
452 comparisons. Agric. For. Meteorol., 313, 108760,
453 <https://doi.org/10.1016/j.agrformet.2021.108760>, 2022.

Formatted: Font: (Default) +Headings (Calibri), 12 pt

454 Hoeltgebaum, L.E.B. and Nelson L.D.: Evaluation of the storage and evapotranspiration terms of
455 the water budget for an agricultural watershed using local and remote-sensing
456 measurements, Agric. For. Meteorol., 341, 109615,
457 <https://doi.org/10.1016/j.agrformet.2023.109615>, 2023.

Formatted: Font: (Default) +Headings (Calibri), 12 pt

458 Lamas Galdo, M.I., Rodriguez García, J.D. and Rebollido Lorenzo, J.M.: Numerical model to
459 analyze the physicochemical mechanisms involved in CO₂ absorption by an aqueous
460 ammonia droplet. Int. J. Environ. Res. Public Health, 18(8), p.4119,
461 <https://doi.org/10.3390/ijerph18084119>, 2021.

Formatted: Font: (Default) +Headings (Calibri), 12 pt

462 Leuning, R.: Estimation of scalar source/sink distributions in plant canopies using lagrangian
463 dispersion analysis: corrections for atmospheric stability and comparison with a
464 multilayer canopy model, Boundary Layer Meteorol., 96:293–314,
465 <https://doi.org/10.1023/A:1002449700617>, 2012.

Formatted: Font: (Default) +Headings (Calibri), 12 pt

466 Massman, W. and Lee, X.: Eddy covariance flux corrections and uncertainties in long-flux
467 studies of carbon and energy exchanges, Agric. For. Meteorol., 113(1–4), 121–144,
468 [https://doi.org/10.1016/S0168-1923\(02\)00105-3](https://doi.org/10.1016/S0168-1923(02)00105-3), 2002.

Formatted: Font: (Default) +Headings (Calibri), 12 pt

469 Mayocchi, C.L. and Bristow, K.L.: Soil surface heat flux: some general questions and comments
470 on measurements, Agric. For. Meteorol., 75(1–3), 43–50 (1995).
471 [https://doi.org/10.1016/0168-1923\(94\)02198-S](https://doi.org/10.1016/0168-1923(94)02198-S), 1995.

Formatted: Font: (Default) +Headings (Calibri), 12 pt

472 McCaughey, J.H. and Saxton, W.L.: Energy balance storage fluxes in a mixed forest, Agric. For.
473 Meteorol., 44(1), 1–18, [https://doi.org/10.1016/0168-1923\(88\)90029-9](https://doi.org/10.1016/0168-1923(88)90029-9), 1988.

Formatted: Font: (Default) +Headings (Calibri), 12 pt

474 Meyers, T. P. and Hollinger, S. E.: An assessment of storage terms in the surface energy balance
475 of maize and soybean, Agric. For. Meteorol., 125(1–2), 105–115,
476 <https://doi.org/10.1016/j.agrformet.2004.03.001>, 2004.

Formatted: Font: (Default) +Headings (Calibri), 12 pt

477 Montagnani, L., Grünwald, T., Kowalski, A., Mammarella, I., Merbold, L., Metzger, S., Sedlák, P.
478 and Siebicke, L.: Estimating the storage term in eddy covariance measurements: the
479 ICOS methodology, *Int. Agrophysics.*, 32 (4), 551–567, <https://doi:10.1515/intag-2017-0037>, 2018.

Formatted: Font: (Default) +Headings (Calibri)

481 Nicolini, G., Aubinet, M., Feigenwinter, C., Heinesch, B., Lindroth, A., Mamadou, O., Moderow,
482 U., Mölder, M., Montagnani, L., Rebmann, C. and Papale, D.: Impact of CO₂ storage flux
483 sampling uncertainty on net ecosystem exchange measured by eddy covariance. *Agri.
484 For. Meteorol.*, 248, 228–239, <http://dx.doi.org/10.1016/j.agrformet.2017.09.025>, 2018.

Formatted: Font: (Default) +Headings (Calibri), 12 pt

485 O'Dell, D., Sauer, T.J., Hicks, B.B., Thierfelder, C., Lambert, D.M., Logan, J. and Eash, N.S.: A
486 short-term assessment of carbon dioxide fluxes under contrasting agricultural and soil
487 management practices in Zimbabwe. *J. Agri. Sci.* 7(3),
488 <http://dx.doi.org/10.5539/jas.v7n3p32>, 2015.

Formatted: Font: (Default) +Headings (Calibri), 12 pt

489 O'Dell, D., Sauer, T.J., Hicks, B.B., Lambert, D.M., Smith, D.R., Bruns, W.A., Basson, A., Marake,
490 M.V., Walker, F., Wilcox, M.D. and Eash, N.S.: Bowen ratio energy balance measurement
491 of carbon dioxide (CO₂) fluxes of no-till and conventional tillage agriculture in Lesotho.
492 *Open J. Soil Sci.* 4(3): 87–97, <http://hdl.handle.net/10919/70228>, 2014.

Formatted: Font: (Default) +Headings (Calibri), 12 pt

493 Oetting, J., Hicks, B. and Eash, N.: On recursive partitioning to refine coordinate rotation in Eddy
494 covariance applications. *Agri. For. Meteorol.*, 1,346:109873,
495 <https://doi.org/10.1016/j.agrformet.2023.109873>, 2024.

Formatted: Font: (Default) +Headings (Calibri), 12 pt

496 Papale, D., Reichstein, M., Aubinet, M., Canfora, E., Bernhofer, C., Kutsch, W. and Yakir, D.:
497 Towards a standardized processing of Net Ecosystem Exchange measured with eddy
498 covariance technique: algorithms and uncertainty estimation, *Biogeosci.*, 3(4), 571–583,
499 <https://doi.org/10.5194/bg-3-571-2006>, 2006.

Formatted: Font: (Default) +Headings (Calibri), 12 pt

500 Pastorello, G., Trotta, C., Canfora, E., Chu, H., Christianson, D., Cheah, Y.W., Poindexter, C.,
501 Chen, J., Elbashandy, A., Humphrey, M. and Isaac, P.: The FLUXNET2015 dataset and the
502 ONEFlux processing pipeline for eddy covariance data. *Sci. Data*, 7(1), 225,
503 <https://doi.org/10.6084/m9.figshare.12295910>, 2020.

Formatted: Font: (Default) +Headings (Calibri), 12 pt

504 Raza, T., Oetting, J., Eash, N., Hicks, B. and Lichiheb, N.: Assessing energy balance closure over
505 maize canopy using multiport system and canopy net storage, in: Proceedings of the
506 104th AMS Annual Meeting, Baltimore, Maryland, USA, 28 January to 1 February, 2024.

507 Raza, T., Hicks, B., Oetting, J. and Eash, N.: On the agricultural eddy covariance storage term:
508 measuring carbon dioxide concentrations and energy exchange inside a maize canopy,
509 in: Proceedings of the 103rd AMS Annual Meeting, Denver, Colorado, USA, 8–12
510 January, 2023.

511 Russell, E.S., Liu, H., Gao, Z., Finn, D. and Lamb, B., Impacts of soil heat flux calculation methods
512 on the surface energy balance closure. Agricultural and Forest Meteorology, 214, 189–
513 200, <https://doi.org/10.1038/nature04514>, 2015.

Formatted: Font: (Default) +Headings (Calibri)

514 Ryan, M., Law, B. Interpreting, measuring, and modeling soil respiration. Biogeochemistry 73,
515 3–27, <https://doi.org/10.1007/s10533-004-5167-7>, 2005.

Formatted: Font: (Default) +Headings (Calibri)

516 Twine, T.E., Kustas, W.P., Norman, J.M., Cook, D.R., Houser, P.R., Meyers, T.P., Prueger, J.H.,
517 Starks, P.J. and Wesely, M.L.: Correcting eddy-covariance flux underestimates over a
518 grassland, Agric. For. Meteorol., 103 (3), 279–300, [https://doi.org/10.1016/S0168-1923\(00\)00123-4](https://doi.org/10.1016/S0168-1923(00)00123-4), 2000.

Formatted: Font: (Default) +Headings (Calibri), 12 pt

520 USDA-NRCS (2018). Soil Survey Staff, Natural Resources Conservation Service, United States
521 Department of Agriculture. Web Soil Survey. Available at:
522 <https://websoilsurvey.sc.egov.usda.gov/App/WebSoilSurvey.aspx>, Accessed November
523 2018.

524 Varmaghani, A., Eichinger, W.E. and Prueger, J.H.: A diagnostic approach towards the causes of
525 energy balance closure problem. Open J. Mod. Hydrol., 6(02), 101,
526 <https://doi.org/10.4236/ojmh.2016.62009>, 2016.

Formatted: Font: (Default) +Headings (Calibri), 12 pt

Formatted: Font: (Default) +Headings (Calibri), 12 pt

527 Verma, S.B. and Rosenberg, N.J.: Vertical profiles of carbon dioxide concentration in stable
528 stratification. Agric. Meteorol, 16(3), 359–369, [https://doi.org/10.1016/0002-1571\(76\)90005-4](https://doi.org/10.1016/0002-1571(76)90005-4), 1976.

Formatted: Font: (Default) +Headings (Calibri), 12 pt

Formatted: Font: (Default) +Headings (Calibri), 12 pt

530 Wang, X., Zhong, L., Ma, Y., Fu, Y., Han, C., Li, P., Wang, Z. and Qi, Y.: Estimation of hourly actual
531 evapotranspiration over the Tibetan Plateau from multi-source data. *Atmos. Res.*, 281,
532 106475, <https://doi.org/10.1016/j.atmosres.2022.106475>, 2023.

Formatted: Font: (Default) +Headings (Calibri), 12 pt

533 Wilson, K.B., Goldstein, A., Falge, E., Aubinet, M., Baldocchi, D., Berbigier, P., Bernhofer, C.,
534 Ceulemans, R., Dolman, H., Field, C., Grelle, A., Ibrom, A., Law, B., Kowalski, A., Meyers,
535 T., Moncrieff, J., Monson, R., Oechal, W., Tenhunen, J., Valentini, R. and Verma, S.:
536 Energy balance closure at FLUXNET sites, *Agric. For. Meteorol.*, 113, 223–243,
537 [https://doi.org/10.1016/S0168-1923\(02\)00109-0](https://doi.org/10.1016/S0168-1923(02)00109-0), 2002.

Formatted: Font: (Default) +Headings (Calibri), 12 pt

Formatted: Font: (Default) +Headings (Calibri), 12 pt